Eur Radiol (2015) 25:2205–2213
DOI 10.1007/s00330-015-3647-x

MOLECULAR IMAGING

Photoacoustic breast tomography prototypes with reported human applications

Jan Menke

Received: 10 September 2014 / Revised: 25 January 2015 / Accepted: 30 January 2015 / Published online: 27 February 2015
© European Society of Radiology 2015

Abstract

Objectives Photoacoustic breast tomography could provide optical molecular imaging with near-infrared light at sonographic image resolution by utilizing the photoacoustic effect. This review summarizes reports about current prototypes that were applied in vivo in humans.

Methods Four databases were searched for reports about prototypes of photoacoustic breast tomography that were tested in vivo in humans. Data extracted from the reports comprised details about system design, phantom studies, and clinical studies.

Results Five prototypes were included. System designs comprised planar, hemicylindrical and hemispherical geometries. In total, 52 of 61 breast cancers (85 %) were detected by three of the prototypes, showing image details such as ring-pattern of the haemoglobin-rich tumour vasculature. A refined prototype provided submillimetre resolution at a good contrast-to-noise ratio up to a depth of about 5 cm in a cup-shaped breast configuration. Another novel prototype demonstrated that in the mammographic imaging geometry, the total imaging depth approximately duplicates with bilateral laser illumination. Most prototypes focused on detecting elevated haemoglobin content related to tumours, but proof-of-principle was also given for multispectral optoacoustic tomography by additional imaging of tissue oxygenation.

Conclusions Photoacoustic breast tomography can detect breast cancer. This radiation-free molecular imaging technology should be further refined and studied for clinical applications.

Electronic supplementary material The online version of this article (doi:10.1007/s00330-015-3647-x) contains supplementary material, which is available to authorized users.

J. Menke (✉)
Radiology Center, University Medical Center, Robert-Koch-Strasse 40, 37075 Goettingen, Germany
e-mail: Menke-J@T-Online.de

Key Points

- *Photoacoustics combines optical imaging with sonographic signal detection.*
- *Photoacoustic tomography could provide molecular imaging at high image resolution.*
- *Prototypes have been designed for human breast cancer imaging.*
- *Preliminary evaluation studies show that photoacoustic tomography detects breast cancer.*
- *This radiation-free method should be further improved and studied for clinical applications.*

Keywords Breast cancer · Photoacoustic tomography · Equipment design · Evaluation studies · Systematic review

Abbreviations and acronyms

DOT	Diffuse optical tomography
MSOT	Multispectral optoacoustic tomography
NIR	Near-infrared
PAT	Photoacoustic tomography
PAM	Photoacoustic mammography

Introduction

Breast cancer is a major health burden, affecting about 12 % of women in Germany [1]. It is the cancer entity with the highest mortality rate (17.8 %) among women in Germany, and its 5-year survival rate is currently about 76 % [1]. These numbers vary among nations [2].

Besides clinical assessment, detection and follow-up of breast cancer is based on imaging. Mammography is the

standard method that can identify tumour-related microcalcifications, soft tissue masses and alterations in the breast architecture [1]. However, particularly in dense breasts of ACR grade III–IV (American College of Radiology), tumours may be hidden in the mammography by parenchyma projecting onto the tumour. Sonography may then help for clarification [3]. It has high image resolution, but limited image contrast. If indicated, gadolinium-enhanced magnetic resonance imaging (MRI) can be added [1, 4, 5]. It has good image contrast and spatial resolution for showing details, such as tumour infiltration into surrounding parenchyma [4], but its availability is limited. A complementary cost-effective imaging method covering the whole breast might therefore be useful in the diagnostic pathway.

Among emerging research methods is molecular imaging with non-ionizing near-infrared (NIR) light [6–14]. In the spectral window of 650–950 nm, the water-related absorption is small [15], so that soft tissue is relatively transparent up to several centimetres in depth. Major endogenous absorbers at 650–950 nm are oxyhaemoglobin and deoxyhaemoglobin, which can alternatively be expressed as the tissue's total haemoglobin content and oxygen saturation [11–14, 16]. This spectral window is also useful for optical contrast agents, such as the human-approved indocyanine green for studying perfusion [17, 18], and optical reporters such as monoclonal antibodies conjugated with gold nanorods or labelled with fluorochromes for tumour-specific imaging [8, 19, 20]. A secondary smaller spectral window with higher total attenuation exists at 1050–1100 nm [15, 16].

Among novel NIR-light-based imaging methods is radiation-free photoacoustic (or optoacoustic) tomography [6–9]. It utilizes the optoacoustic (or photoacoustic) effect, described by Bell, Röntgen, and others [21, 22]. In principle, if a short near-infrared (NIR) light pulse, e.g., of some nanoseconds duration, is absorbed by a small molecular target, then the target's initial thermoelastic expansion generates exponentially, decaying broadband acoustic pressure waves that can be measured by ultrasound detectors for generating images. In photoacoustic tomography, the image contrast is determined by optical absorption, while image resolution is determined by ultrasound. Therefore, it can potentially provide molecular imaging at high image resolution. Further details are provided in Supplementary Material 1.

Photoacoustic tomography is becoming useful for preclinical imaging [7, 8], and is being translated to human applications such as photoacoustic breast tomography, which is named "photoacoustic mammography" (PAM) in the following. PAM could be used for primary diagnosis, treatment assessment during neoadjuvant chemotherapy, and follow-up of breast cancer [23–27]. If further development is successful, then PAM could be used for imaging the whole breast, with a focus on haemoglobin-rich vascularized tumours, supplemented by dynamic contrast-enhancement by intravenous indocyanine green and potentially by tumour-specific optical reporters. In this regard, it may have some properties of magnetic resonance mammography, and some novel molecular imaging properties that are currently not provided by other methods. However, PAM is just being developed, so that a detailed comparison to other breast imaging methods is not possible at this stage. For presenting this novel research technology to clinical radiologists, this systematic review summarizes reports about current PAM prototypes that were applied in vivo in humans.

Methods

Data sources and study selection

The PubMed, Scopus, Biosis and Web of Science databases were searched for "photoacoustic or optoacoustic" and "breast or mammo* or tomography or tomographic" and related terms without language restrictions (Fig. 1). Additionally, reference lists of retrieved articles were searched. Eligible studies had applied a PAM prototype in vivo in humans.

Data extraction

Several data about the PAM prototypes were extracted from the publications, comprising details about system design, phantom studies, and clinical studies.

Breast thickness at mammography

For the discussion, the compressed breast thickness of 1000 digital mammography images at the University Medical Center Goettingen were extracted from the DICOM headers by a proprietary program written in C++ (Microsoft) by the author.

Results

Data sources

The literature search identified 1519 items (Fig. 1). After excluding duplicates and reading titles and abstracts, the full text of 45 items was assessed. Nine articles were finally included, describing five different PAM prototypes [25–30].

Excluded reports

Among excluded articles were 20 reports about photoacoustic tomography systems that had not been tested in vivo in humans. Among them were four hybrid systems that combined photoacoustic tomography (PAT)

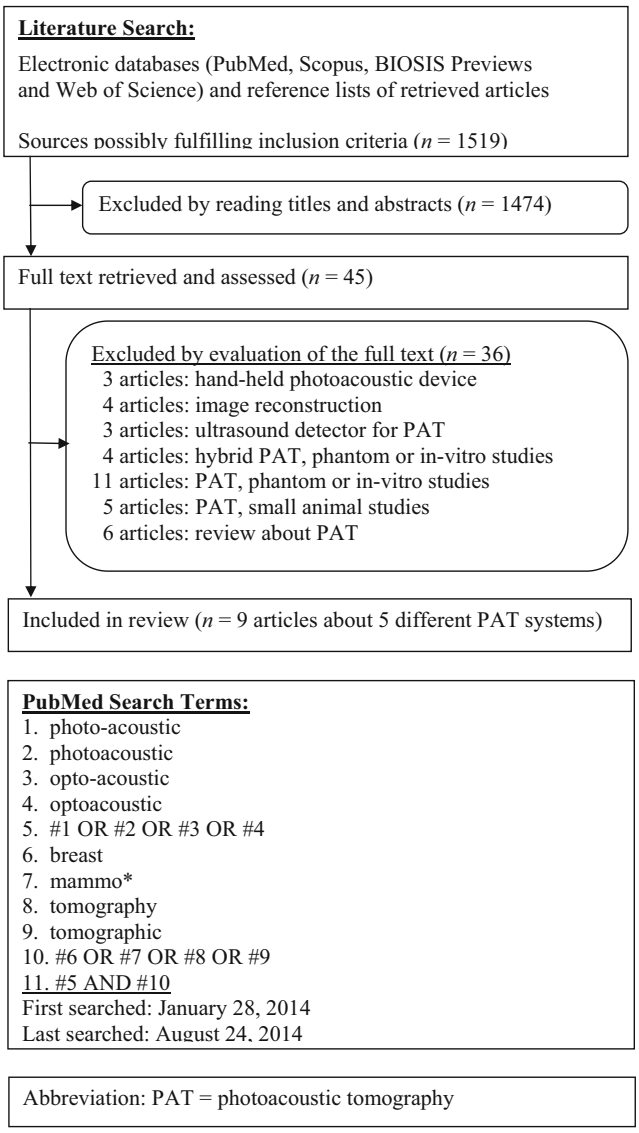

Fig 1 Literature search and selection

with diffuse optical tomography (DOT) [31, 32] or with thermo-acoustic tomography (TAT) [33, 34].

Included reports

In the temporal order of publication, the five included PAM prototypes are the "Twente Photoacoustic Mammoscope" (Twente PAM) [23, 24, 35, 36], "Laser Optoacoustic Imaging System" (LOIS-64) [26], 128-detector OptoSonics photoacoustic mammography system (OptoSonics-128 PAM) [29], Canon photoacoustic mammography system (Canon PAM) [25, 28], and the refined 512-detector OptoSonics photoacoustic mammography system (OptoSonics-512 PAM) [30]. Details are provided in Supplementary Material 2 and in the following.

Twente PAM

This was the first PAM prototype with in vivo reports in human breast cancer [23, 24, 35, 36]. The patient is lying in prone position with a breast gently compressed in the mammographic geometry (Fig. 2a and b). Pulsed NIR laser light (1064 nm, 5–10 nanosecond pulses at 10 Hz, laser output 60 mJ) illuminates about 2.5 cm^2 of skin at about 25 mJ/cm^2 per pulse in transmission mode. The 590-element ultrasound detector array (central frequency 1 MHz) has 2×2 mm sized elements at a distance of 3.2 mm. Due to only one receiver channel, the elements were sequentially read, and imaging a breast area of 37×31 mm (thickness about 15–60 mm) by 12×10 detector elements required about 20 minutes with signal averaging. Lateral image resolution was 3.1–4.4 mm and depth resolution 3.2–3.9 mm. Thirty patients were prospectively studied in 2007 and 2010/2011 [23, 24]. Twelve patients were excluded for technical or patient-related reasons, such as poor acoustic breast-detector coupling or cancer outside the field of view. Among the 18 included patients, 14 of 15 breast cancers were correctly detected. As far as reported, on average, the tumours were about 30 mm in size at about a depth of 15 mm [23, 24]. A sonographic tumour depth of >30 mm (shortest skin−tumour distance) was also reported [24]. The published images show details such as a ring-pattern in invasive ductal carcinoma (Fig. 3) [23]. High image intensity represents high haemoglobin content from tumour vascularization. Three other patients had benign cysts imaged by PAM [23, 24].

Canon PAM

The Canon PAM shares similarities with the Twente PAM, such as mammographic imaging geometry, but several details differ (Fig. 2c and d) [28]. The Canon PAM has one ultrasound detector, but utilizes bilateral laser illumination from the detector side (reflection) and opposed side (transmission). Total imaging depth therefore approximately duplicates, compared to unilateral illumination (Fig. 4a in [28]). About 9 cm^2 of skin is illuminated at ≤9 mJ/cm^2 (transmission) or 3 mJ/cm^2 (reflection) per pulse by two lasers (output 80 mJ). They are tuneable at 700–900 nm, allowing for multispectral optoacoustic tomography (MSOT) by using different wavelengths and spectral unmixing. This was done at 756 nm and 797 nm for imaging of oxygen saturation and total haemoglobin content. The ultrasound detector (central frequency 1 MHz) has 345 (15×23) elements, each sizing 2×2 mm. Lateral image resolution is 2–3 mm. Parallel data acquisition allowed for imaging a 30×46 mm scan area in 45 seconds. Thirty-one patients were studied prospectively in 2010/2011. Five patients were excluded for technical or patient-related reasons. Among included patients, 20 of 26 breast cancers were correctly detected. In these tumours, the

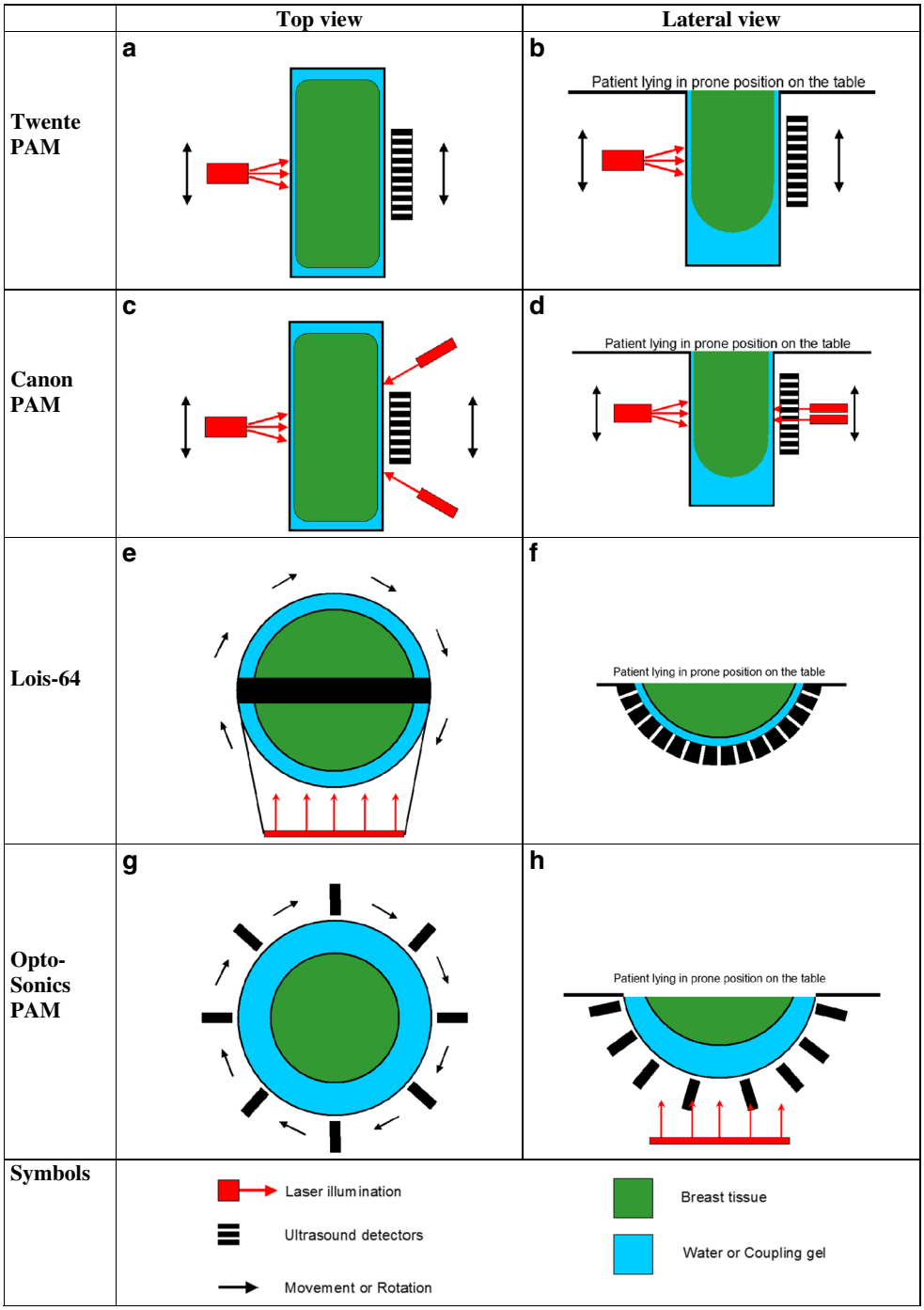

Fig 2 PAM designs. This figure shows the design principles of the PAM prototypes with top view (*left column*) and lateral view (*right column*). In all systems, the patient is lying in prone position on a table with one breast inserted into a holding-and-measurement device below the table. ***Twente PAM*** (**a**, **b**): The breast is gently compressed in the mammographic geometry. The laser-detector unit can be moved vertically and/or laterally to the region of interest, where PAM measurements are performed in the transmission mode, with laser illumination from one side and ultrasound detection at the opposed side. ***Canon PAM*** (**c**, **d**): In addition to the Twente design, the compressed breast is also illuminated from the detector side (reflection mode) by two off-axis laser beams that are located laterally to the detectors. Other technical details also differ from the Twente PAM. ***LOIS-64*** (**e**, **f**): The uncompressed breast is inserted into a hemicylindrical cup (**f**). The arc-shaped ultrasound detector array (**f**) can rotate (**e**) around that cup to cover the whole breast by several two-dimensional PAM images at different angles of rotation. The breast is illuminated horizontally, perpendicular to the detector arc (**e**). ***OptoSonics-128 and -512 PAM*** (**g**, **h**): The breast is placed into a plastic cup and is thereby self-compressed into a relatively flat shape (**h**). This plastic cup is located within a water-filled imaging bowl that is illuminated from the bottom (**h**). The ultrasound detector elements surround the bowl in a spiral pattern. The number of radial projections can be increased by rotating (**g**) the bowl around its vertical axis

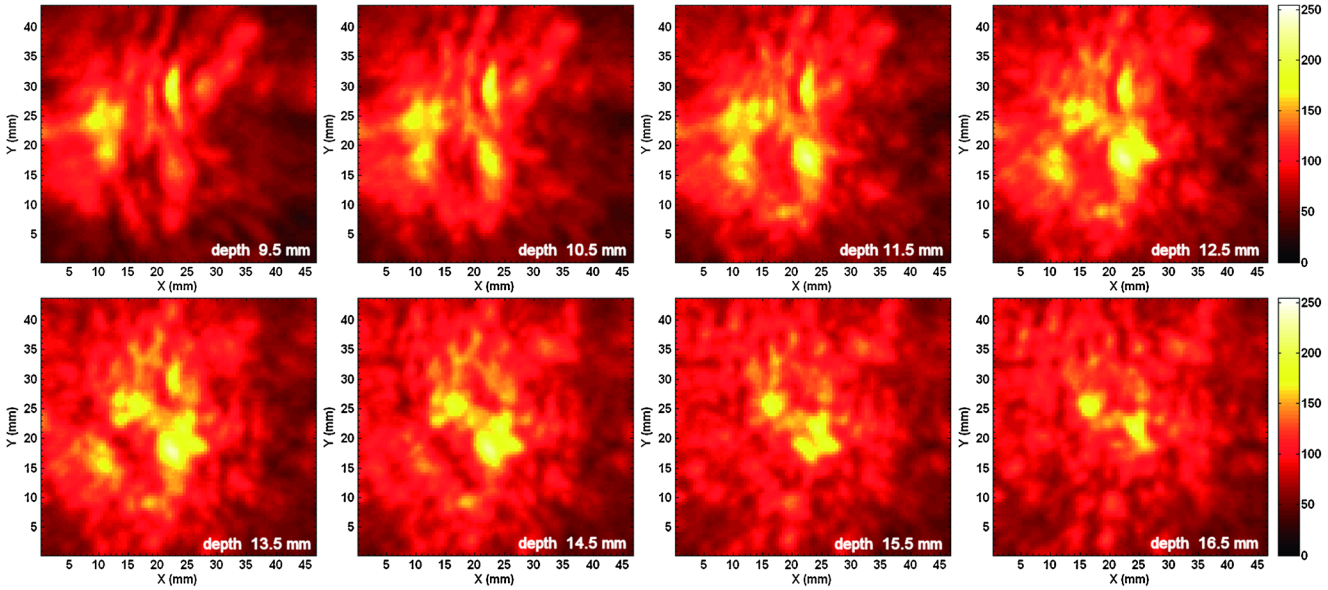

Fig. 3 PAM images in a patient with invasive ductal carcinoma. These images were acquired with the Twente PAM in a "57-year-old woman with invasive ductal carcinoma exhibiting neuroendocrine differentiation in the right breast. Selected slice images of photoacoustic reconstructed data set in craniocaudal view. The inter-slice spacing is 1 mm, with the first slice 9.5 mm below the illuminated breast surface. The ring pattern of higher intensity, which depicts strong vascularization at the tumour periphery, is evident in the slices at depths 11.5 to 14.5 mm". Reprinted with permission from Fig. 6 of S. Manohar et al,, Opt Express 2007 (with additional depth labels) [23]

mean oxygen saturation was measured as 78.6 % (range, 53.7–100 %), and mean haemoglobin content was measured as 207 μM (87–309 μM). Average tumour size was 20 mm. Tumour depth was reported up to 28 mm beneath the skin at a compressed breast thickness of 68 mm [25]. The corresponding PAM image showed haemoglobin-related high-intensity signals in the tumour, although its margins were less well defined compared to those from MRI (Fig. 4 in [25]).

LOIS-64 PAM

In a prone position, an uncompressed breast was inserted into a hemicylindrical cup (Fig. 2e and f) [26]. An arc-shaped ultrasound detector array (central frequency 1.25 MHz) can rotate around that cup. The breast is illuminated perpendicular to the arc by a pulsed Q-switched Alexandrite laser (757 nm) having a high output of ≤750 mJ. A large skin area is illuminated, so that the skin's maximum illumination is just about 10 mJ/cm^2 per pulse. The 19-cm–long, arc-shaped ultrasound detector has a width of 2 cm and consists of 64 anisotropic rectangular elements, each sizing 3×20 mm. The resulting 20-mm–thick, two-dimensional images have depth resolution of about 0.5 mm. Arc rotation results in three-dimensional breast coverage. In 27 patients, a total of 34 breast lesions were prospectively studied. Six lesions were excluded for technical reasons. Eight of the included lesions were benign, and 18 of 20 cancer lesions were detected by PAM. Tumour size was 11–26 mm, and maximum reported tumour depth was 26 mm. In the published PAM images, the tumours showed high haemoglobin-related image contrast, indicating tumour vascularization (Figs. 16 and 17 in [26]). Depiction of fine details was limited, probably due to the 20-mm thickness of the image slices.

OptoSonics-128 PAM

In prone position, a breast was placed into a plastic cup that is optically and acoustically transparent (Fig. 2g and h). A water-filled imaging bowl with a100-mm radius surrounds the cup. The bowl is illuminated from the bottom by a tuneable (680–950 nm) optical parametric oscillator (OPO) laser system (output 20 mJ, 10 Hz). About 20 cm^2 of skin is illuminated at just about 1 mJ/cm^2 per pulse. A total of 128 ultrasound detector elements (central frequency 5 MHz) are located around the bowl, each sizing 3×3 mm. Rotating the detector array around its vertical axis results in increased sampling projections with a spiral scan pattern. Three-dimensional PAM images of a human volunteer at 800 nm were reported as having submillimetre resolution up to 40 mm penetration depth [29].

OptoSonics-512 PAM

This refined system (Fig. 2g and h) has 512 detector elements; can image larger breasts; the central detector frequency is decreased to 2 MHz; a single-wavelength Alexandrite laser (756 nm) is used; maximum laser output is increased to 300 mJ, and thereby the skin's illumination increased to 10 mJ/cm^2 per pulse; imaging depth increased to about 5 cm; and image resolution is 0.42 mm. In phantom

experiments, the image contrast decreased exponentially at increasing depth, as expected (Fig. 9a in [30]). The image noise also decreased with depth. Therefore, below 30 mm depth, the contrast-to-noise ratio (CNR) was approximately constant (~200) and was limited by streak noise. For greater depths up to 5.3 cm, the system's electronic noise began to degrade the CNR (Fig. 9b in [30]). For covering the whole breast, the largest spiral acquisition (240 mm diameter) required about 3.2 min. In four healthy volunteers, the breast vasculature was visualized at submillimetre resolution up to a penetration depth of about 5 cm from the skin to the chest wall [30].

Sensitivity for breast cancer detection

In total, 52 of 61 breast cancers (85 %) were detected by the Twente, Canon and LOIS-64 PAMs among the included patients [23–26].

Exclusion of patients/lesions

In total, 23 further patients/lesions had been excluded from analysis [23–26]. The reasons comprised eight cases with "small breast size or region-of-interest too close to the chest wall" in PAMs with mammographic imaging geometry, five cases with "poor acoustic coupling between breast and ultrasound detector", five cases with "system malfunction", three cases with "patient discomfort or lesion not completely imaged", and two cases with "operator error".

Breast thickness at mammography

At mammography, the average compressed thickness of 1000 breasts at the University Center Goettingen was about 5.6 cm (2.5 percentile: 3.1 cm; 97.5 percentile: 8.3 cm).

Imaging examples

For illustration, some PAM images are reprinted with permission (Figs. 3 and 4) [23, 30].

Discussion

General comments

Photoacoustic breast tomographic has been possible with the presented PAM prototypes. Breast cancers showed high image contrast at PAM, due to haemoglobin-rich vascularization. Currently, the OptoSonics-512 PAM and Canon PAM seem to be the most technically advanced prototypes.

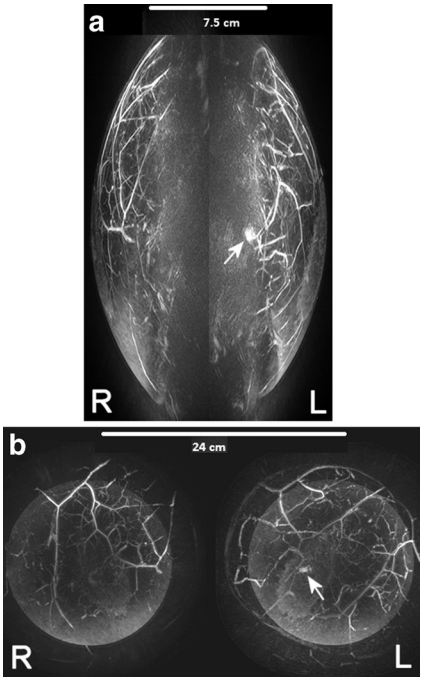

Fig. 4 PAM images of the breast vasculature in a healthy volunteer. Photoacoustic mammography with the OptoSonics PAM-512 in a healthy woman (R = right breast; L = left breast). Panel *A* shows medio-lateral maximum intensity projections (MIP) of the haemoglobin-rich breast vasculature, and panel *B* shows coronal MIPs. The small oval lesion in the central left breast (*arrows*) is located at a depth of 45 mm beneath the skin (personal communication with R.A. Kruger). Reprinted with permission from Figs. 11-2 and 12-2 of R.A. Kruger et al., Med Phys 2013 (with additional scale bars and markers) [30]

Imaging geometries

Radial-projection geometries are utilized two-dimensionally by the LOIS-64 PAM and three-dimensionally by the OptoSonics PAMs [26, 29, 30]. Contrarily, the Twente PAM applies a planar geometry in transmission mode [23, 24, 35, 36]. The Canon allows for the study of benefits and limitations of transmission versus reflection in a planar geometry [25, 28]. Further research is required to determine which imaging geometry might be best.

Laser energy and illumination area

The skin's maximum permitted laser illumination is defined by DIN EN 60 825-1 and corresponding American National Standards Institute (ANSI) standards (Supplementary Material 1) [37]. These limits increase from 20 mJ/cm^2 at 650 nm to 100 mJ/cm^2 at 1050 nm for single laser pulses at 10 Hz. All PAM prototypes operated well below these limits. Particularly at higher wavelengths, a higher incident laser energy density would have been permitted. The illuminated skin area is not limited and may be large for imaging the whole breast, as done in the OptoSonics-512 PAM (Supplementary Material 2). In

the other PAM systems, the imaged breast volume is currently relatively small. It may be expected that illuminating a large skin area at a relatively high but permitted incident laser energy [37] provides a maximum of optoacoustic signals for image generation. In that regard, a full breast illumination might be best for a fast whole-breast PAM system, but regional imaging is also possible for prototype development.

Penetration depth of the NIR light

In the OptoSonics-512 PAM, the NIR light's penetration depth of about 5 cm at unilateral illumination is considered sufficient for imaging up to 90 % of women in the USA [30], since the breast is relatively flat when self-compressed in the prone position. If that penetration depth becomes possible in the Canon PAM, then the total depth of $2 \times 5 = 10$ cm with bilateral illumination would be sufficient for imaging most women in the mammographic geometry.

Ultrasound detectors

Most detectors had 2×2 to 3×3 mm sized elements. In the OptoSonics PAMs, the bowls' radial-arranged detector elements are distant from the cup-inset, thus representing smaller sizes when projected on the breast surface. In the PAM system with the highest spatial resolution and penetration depth (OptoSonics-512 PAM), the broadband ultrasound detector had a central frequency of 2 MHz with a bandwidth of 70 %. Development of specific detectors may help in generating high-resolution images with a good contrast-to-noise ratio [38]. Currently, only the OptoSonics PAMs provide a submillimetre resolution that is sufficient for showing small imaging details similar to magnetic resonance mammography.

Image reconstruction

Most PAM systems applied backprojection algorithms for image reconstruction. For more quantitative imaging, the reconstruction problem can be divided into generating a high-resolution map of the tissue's optical absorption coefficients μa and a low-resolution map of local light fluence U (Supplementary Material 1). In the breast with its relatively homogeneous composition (fatty and glandular soft tissue, no air, no bones), the generation of that low-resolution map is perhaps more easy than in the heterogeneous tissue of mice (soft tissue, lungs, bones) in preclinical studies.

Multispectral optoacoustic tomography (MSOT)

Most PAMs provided only single-wavelength images with contrast dominated by haemoglobin. However, MSOT is required for spectral decomposition of optical absorbers [39, 40]. The Canon PAM applied MSOT for generating additional images of tissue oxygenation. Differentiating fat from water [15, 41] might also be useful for correlation with T1- weighted and T2-weighted MRI images. Molecular and functional MSOT imaging with tumour-specific optical reporters [8, 19, 20] or dynamic contrast enhancement with indocyanine green [18] has already been shown in preclinical studies.

Image quality

According to phantom experiments and imaging in healthy volunteers, the OptoSonics-512 PAM currently shows the best image quality with submillimetre resolution and a good contrast-to-noise ratio [30]. Its performance in a clinical setting needs to be studied. At lower image resolution, breast cancers were detectable by the other PAM prototypes [23–26]. Refining their image quality would allow for evolution of different system designs and could increase the diagnostic accuracy in image interpretation.

Comparison to diffuse optical tomography (DOT)

Breast DOT shows that NIR light can transmit the whole breast and is still detectable [10, 11]. The haemoglobin-related image contrast is good, but image resolution is low due to diffuse photon scattering [11]. Nevertheless, DOT can detect breast cancer [10]. In hybrid PAM/DOT systems, low-resolution maps of optical absorption from DOT could provide a priori information in the generation of quantitative PAM images [31, 32].

Comparison to hand-held photoacoustic devices

Hand-held photoacoustic devices were excluded in this review, since they do not represent a tomography system that could automatically cover the whole breast. However, hand-held devices are also very promising since they are portable, cheap, and can be combined with ultrasound in a hybrid system [42–47]. Basically, hand-held photoacoustic devices are not concurrent, but are complementary to PAM. For example, in a patient with mammographically dense breasts, PAM might detect a tumour-suspicious lesion, and handheld photoacoustic-sonography imaging could then be used for guiding a biopsy, if clinically indicated.

Research on photoacoustic macroscopic imaging

The human breast is particularly suitable for translation of preclinical photoacoustic methods to large human organs: Breast cancer is frequent, some cancers are difficult-to-detect with standard imaging, and the breast is well accessible and can be transmitted by NIR light as shown by DOT, and does not contain bones or air that hinders ultrasound.

Technical limitations and potentials of PAM

Based on the published experience, the following problems should be considered for the design of future PAM prototypes: In the mammographic imaging geometry (Twente PAM and Canon PAM), the breasts of some patients were too small to be imaged, and in other patients, the region of interest was too close to the chest wall [23–25]; this is essentially the same problem as in mammography. In the hemicylindrical or hemispherical imaging geometry (LOIS-64 and OptoSonics PAM), this is in principle no problem if the system's penetration depth is sufficient [26, 29, 30]. The penetration depth of the OptoSonics-512 PAM is already considered suitable for imaging 90 % of women [30], and further development is suggested for imaging all breast sizes. Close acoustic coupling between skin and the ultrasound detector is required to avoid erroneous optoacoustic signals; this is essentially the same as in standard sonography. In some PAM prototypes, the imaging time was rather long, but the recent prototypes are already much faster, owing to the well-known advances in computer technology and microtechnology. The current studies showed that invasive ductal carcinoma (IDC), invasive lobular carcinoma (ILC), ductal carcinoma in situ (DCIS) and different benign conditions could be imaged by PAM. This potential for breast cancer detection should be assessed by further studies with refined PAM systems. Molecular imaging with tumour-specific markers may offer further potentials for cancer detection and treatment response assessment.

Advantages, disadvantages and contraindications of PAM, compared to other methods

Particularly in dense breasts, PAM could be used to detect tumours that are not obvious in the mammography. PAM could detect vascularized tumours by their elevated haemoglobin content, and by their perfusion characteristics when using indocyanine green. Fatty tissue, cysts and oedema could also be depicted when imaging at multiple suitable NIR wavelengths. These MRI-like soft-tissue imaging properties could be offered to a large number of patients, since costs of a PAM instrument would be small compared to MRI. However, the PAM images will require qualified interpretation, thus increasing the workload for radiologists and other breast imaging specialists, when offering PAM to many patients. Compared to sonography, PAM adds molecular imaging properties, and a hybrid PAM/sonography system could provide both imaging characteristics. Compared to diffuse optical imaging, PAM can potentially provide the high image resolution that is required for depicting details such a tumour's infiltration into its surroundings. PAM is free of ionizing radiation, which is an advantage over any radiation-based method. Even microcalcifications might be detected by PAM [48], but mammography is the gold standard for this purpose. Currently, PAM has no known contraindications.

Conclusion

Photoacoustic breast tomography is a promising method for gaining complementary molecular information about breast tumours. This radiation-free technology should be further improved to study its potential for clinical breast cancer imaging.

Acknowledgments The scientific guarantor of this publication is Jan Menke. The author of this manuscript declares no relationships with any companies, whose products or services may be related to the subject matter of the article. The author states that this work has not received any funding. No complex statistical methods were necessary for this paper. Institutional Review Board approval was not required because this is a review. Written informed consent was not required for this study because this is a review. Some study subjects or cohorts have been previously reported in the cited papers. Methodology: systematic review.

References

1. Kreienberg R, Kopp I, Albert U et al (2008) German Cancer Society and German Society for Gynecology and Obstetrics. Interdisciplinary S3 guidelines for the diagnosis, treatment and follow-up care of breast cancer, 1st updated version 2008. ISBN 978-3-88603-948-7
2. Youlden DR, Cramb SM, Dunn NA, Muller JM, Pyke CM, Baade PD (2012) The descriptive epidemiology of female breast cancer: an international comparison of screening, incidence, survival and mortality. Cancer Epidemiol 36:237–248
3. Weigel S, Biesheuvel C, Berkemeyer S, Kugel H, Heindel W (2013) Digital mammography screening: how many breast cancers are additionally detected by bilateral ultrasound examination during assessment? Eur Radiol 23:684–691
4. Peters NH, Borel Rinkes IH, Zuithoff NP, Mali WP, Moons KG, Peeters PH (2008) Meta-analysis of MR imaging in the diagnosis of breast lesions. Radiology 246:116–124
5. Pediconi F, Kubik-Huch R, Chilla B, Schwenke C, Kinkel K (2013) Intra-individual randomised comparison of gadobutrol 1.0 M versus gadobenate dimeglumine 0.5 M in patients scheduled for preoperative breast MRI. Eur Radiol 23:84–92
6. Wang LV, Hu S (2012) Photoacoustic tomography: in vivo imaging from organelles to organs. Science 335:1458–1462
7. Ntziachristos V (2010) Going deeper than microscopy: the optical imaging frontier in biology. Nat Methods 7:603–614
8. Ntziachristos V, Razansky D (2010) Molecular imaging by means of multispectral optoacoustic tomography (MSOT). Chem Rev 110: 2783–2794
9. Wang LV (2008) Prospects of photoacoustic tomography. Med Phys 35:5758–5767
10. Leff DR, Warren OJ, Enfield LC et al (2008) Diffuse optical imaging of the healthy and diseased breast: a systematic review. Breast Cancer Res Treat 108:9–22
11. Pogue BW, Jiang S, Dehghani H et al (2004) Characterization of hemoglobin, water, and NIR scattering in breast tissue: analysis of intersubject variability and menstrual cycle changes. J Biomed Opt 9: 541–552
12. Menke J, Voss U, Möller G, Jorch G (2003) Reproducibility of cerebral near infrared spectroscopy in neonates. Biol Neonate 83:6–11

13. Menke J, Stöcker H, Sibrowski W (2004) Cerebral oxygenation and hemodynamics during blood donation studied by near-infrared spectroscopy. Transfusion 44:414–421
14. Menke J, Möller G (2014) Cerebral near-infrared spectroscopy correlates to vital parameters during cardiopulmonary bypass surgery in children. Pediatr Cardiol 35:155–163
15. Hale GM, Querry MR (1973) Optical constants of water in the 200-nm to 200-microm wavelength region. Appl Opt 12:555–563
16. Kuenster JT, Norris KH (1994) Spectrophotometry of human haemogobin in the near infrared region from 620 to 2500 nm. J Near Infrared Spectrosc 2:59–65
17. Landsman ML, Kwant G, Mook GA, Zijlstra WG (1976) Light-absorbing properties, stability, and spectral stabilization of indocyanine green. J Appl Physiol 40:575–583
18. Herzog E, Taruttis A, Beziere N, Lutich AA, Razansky D, Ntziachristos V (2012) Optical imaging of cancer heterogeneity with multispectral optoacoustic tomography. Radiology 263:461–468
19. Sano K, Mitsunaga M, Nakajima T, Choyke PL, Kobayashi H (2012) In vivo breast cancer characterization imaging using two monoclonal antibodies activatably labeled with near infrared fluorophores. Breast Cancer Res 14:R61
20. Li PC, Wang CR, Shieh DB et al (2008) In vivo photoacoustic molecular imaging with simultaneous multiple selective targeting using antibody-conjugated gold nanorods. Opt Express 16:18605–18615
21. Bell AG (1880) On the production and reproduction of sound by light. Am J Sci 118:305–324
22. Röntgen WC (1881) On tones produced by the intermittent irradiation of a gas. Philos Mag (Ser 5) 68:308–311
23. Manohar S, Vaartjes SE, van Hespen JC et al (2007) Initial results of in vivo non-invasive cancer imaging in the human breast using near-infrared photoacoustics. Opt Express 15:12277–12285
24. Heijblom M, Piras D, Xia W, van Hespen JC et al (2012) Visualizing breast cancer using the Twente photoacoustic mammoscope: What do we learn from twelve new patient measurements? Opt Express 20: 11582–11597
25. Kitai T, Torii M, Sugie T et al (2014) Photoacoustic mammography: initial clinical results. Breast Cancer 21:146–153
26. Ermilov SA, Khamapirad T, Conjusteau A et al (2009) Laser optoacoustic imaging system for detection of breast cancer. J Biomed Opt 14:024007
27. Jiang S, Pogue BW, Carpenter CM et al (2009) Evaluation of breast tumor response to neoadjuvant chemotherapy with tomographic diffuse optical spectroscopy: case studies of tumor region-of-interest changes. Radiology 252:551–560
28. Fukutani K, Someda Y, Taku M et al (2011) Characterization of photoacoustic tomography system with dual illumination. Proc SPIE 7899:78992J1–78992J7
29. Kruger RA, Lam RB, Reinecke DR, Del Rio SP, Doyle RP (2010) Photoacoustic angiography of the breast. Med Phys 37:6096–6100
30. Kruger RA, Kuzmiak CM, Lam RB, Reinecke DR, Del Rio SP, Steed D (2013) Dedicated 3D photoacoustic breast imaging. Med Phys 40: 113301
31. Li X, Xi L, Jiang R, Yao L, Jiang H (2011) Integrated diffuse optical tomography and photoacoustic tomography: phantom validations. Biomed Opt Express 2:2348–2353
32. Xi L, Li X, Yao L, Grobmyer S, Jiang H (2012) Design and evaluation of a hybrid photoacoustic tomography and diffuse optical tomography system for breast cancer detection. Med Phys 39:2584–2594
33. Ku G, Fornage BD, Jin X, Xu M, Hunt KK, Wang LV (2005) Thermoacoustic and photoacoustic tomography of thick biological tissues toward breast imaging. Technol Cancer Res Treat 4:559–566
34. Pramanik M, Ku G, Li C, Wang LV (2008) Design and evaluation of a novel breast cancer detection system combining both thermoacoustic (TA) and photoacoustic (PA) tomography. Med Phys 35:2218–2223
35. Manohar S, Kharine A, van Hespen JC, Steenbergen W, van Leeuwen TG (2005) The Twente Photoacoustic Mammoscope: system overview and performance. Phys Med Biol 50:2543–2557
36. Manohar S, Kharine A, van Hespen JC, Steenbergen W, van Leeuwen TG (2004) Photoacoustic mammography laboratory prototype: imaging of breast tissue phantoms. J Biomed Opt 9:1172–1181
37. DIN EN 60 825-1 (VDE 0837-1): 200−11
38. Rosenthal A, Razansky D, Ntziachristos V (2011) High-sensitivity compact ultrasonic detector based on a pi-phase-shifted fiber Bragg grating. Opt Lett 36:1833–1835
39. Glatz J, Deliolanis NC, Buehler A, Razansky D, Ntziachristos V (2011) Blind source unmixing in multi-spectral optoacoustic tomography. Opt Express 19:3175–3184
40. Razansky D, Buehler A, Ntziachristos V (2011) Volumetric real-time multispectral optoacoustic tomography of biomarkers. Nat Protoc 6: 1121–1129
41. van Veen RL, Sterenborg HJ, Pifferi A, Torricelli A, Chikoidze E, Cubeddu R (2005) Determination of visible near-IR absorption coefficients of mammalian fat using time- and spatially resolved diffuse reflectance and transmission spectroscopy. J Biomed Opt 10:054004
42. Haisch C, Eilert-Zell K, Vogel MM, Menzenbach P, Niessner R (2010) Combined optoacoustic/ultrasound system for tomographic absorption measurements: possibilities and limitations. Anal Bioanal Chem 397:1503–1510
43. Dean-Ben XL, Razansky D (2013) Portable spherical array probe for volumetric real-time optoacoustic imaging at centimeter-scale depths. Opt Express 21:28062–28071
44. Kim C, Erpelding TN, Jankovic L, Pashley MD, Wang LV (2010) Deeply penetrating in vivo photoacoustic imaging using a clinical ultrasound array system. Biomed Opt Express 1:278–284
45. Dean-Ben XL, Razansky D (2013) Functional optoacoustic human angiography with handheld video rate three-dimensional scanner. Photoacoustics 1:68–73
46. Daoudi K, van den Berg PJ, Rabot O et al (2014) Handheld probe integrating laser diode and ultrasound transducer array for ultrasound/photoacoustic dual modality imaging. Opt Express 22:26365–26374
47. Jaeger M, Preisser S, Kitz M et al (2011) Improved contrast deep optoacoustic imaging using displacement-compensated averaging: breast tumour phantom studies. Phys Med Biol 56:5889–5901
48. Kang J, Kim EK, Kim GR, Yoon C, Song TK, Chang JH (2015) Photoacoustic imaging of breast microcalcifications: a validation study with 3-dimensional ex vivo data and spectrophotometric measurement. J Biophotonics 8:71–80